High resolution detection of fluorescently labeled microorganisms in environmental samples using time-resolved fluorescence microscopy

Russell Connally [a,*], Duncan Veal [a], James Piper [b]

[a] *Centre for Fluorometric Applications in Biotechnology, Department of Biological Sciences, Macquarie University, Sydney, NSW 2109, Australia*
[b] *Centre for Laser Applications, Department of Physics, Macquarie University, Sydney, NSW 2109, Australia*

Abstract

The high level of discrimination offered by fluorescence microscopy has led to its widespread use for the analysis of individual microbial cells. The major limitation of fluorescence microscopy in microbial ecology is that many types of environmental samples contain autofluorescent material that can obscure emission from a fluorescent label. Time-resolved fluorescence microscopy (TRFM) is a technique that greatly reduces background autofluorescence whilst maintaining signal strength of the fluorescent target. TRFM differs from fluorescent microscopy in the use of fluorophores that are characterized by long-lived luminescence. Samples are briefly illuminated to excite fluorescence then capture of luminescence is delayed for a time interval sufficient to ensure autofluorescence has largely faded. TRFM has not been extensively used in microbiology because of the limitations and cost of available time-resolved microscopes and the lack of suitable long-lived fluorescent labels. Here we describe modification of a commercial fluorescence microscope for time-resolved operation through the addition of an image-intensified camera and low cost flashlamp. The TRFM was used in combination with a novel immunofluorophore for the specific detection of *Giardia* cysts in a water sample containing large amounts of autofluorescent material. A 60-μs gate delay between excitation and detection resulted in a 30-fold increase in contrast of labeled parasites compared to conventional immunostaining. To our knowledge, this is the first report of the use of TRFM for the detection of microorganisms in environmental samples. © 2002 Federation of European Microbiological Societies. Published by Elsevier Science B.V. All rights reserved.

Keywords: Time-resolved fluorescence microscopy; Lanthanide; Chelate; *Giardia*

1. Introduction

Fluorescence-based microscopy techniques are widely used in microbial ecology. Such techniques include fluorescence staining for total counts, viability counts, immunofluorescence staining and fluorescence in situ hybridization (FISH) [1]. Whilst fluorescence provides superior discrimination over chromophore-based techniques, its applicability is limited in situations where a weak fluorescent signal must be viewed against high levels of sample autofluorescence.

To reduce autofluorescence, narrow band-pass filters can be used to spectrally resolve fluorophores. This approach however is unable to assist in the (frequent) instance when autofluorescence occurs within the same passband as the target fluorophore.

For example, immunofluorescence is routinely used for the analysis of water samples for *Cryptosporidium* and *Giardia*. Autofluorescent algae and mineral particles present in environmental water sources can result in false positives, obscure immunofluorescence and greatly increase the tedium of analysis [2,3]. Background autofluorescence has been reported to be a significant limitation in the use of FISH techniques for analysis of microbial communities in activated sludge [4], soil [5] and seawater (Cavicchioli, R., University of NSW, Australia, personal communication).

The underlying principle exploited in time-resolved methods is the rapid decay of autofluorescence compared to the typical lifetime of a long-lived synthetic fluorophore, see Fig. 1. An intense light pulse of short duration that decays rapidly to zero intensity is used to excite fluorescence in the sample. The period of time that elapses from excitation to capture (gate delay period) is set to detect only the long-lived emissions. During this time, autofluorescence decays rapidly to low levels yet the long-

* Corresponding author. Tel.: +61 (2) 9850 8111.
E-mail address: rconnall@ics.mq.edu.au (R. Connally).

lived fluorophore decays only minimally, thus greatly increasing the signal to noise (S/N) ratio. Autofluorescence of most natural compounds is characterized by fluorescent lifetimes ranging from 1 to 100 ns whereas fluorophores are now available with lifetimes greater than 1.6 ms [6]. Time-resolved methods exploit the large difference in fluorescence decay lifetimes between natural autofluorophores and long-lived synthetic fluorophores.

A commercial epifluorescence microscope can be readily modified to exploit the fluorescence lifetime differential through the addition of a pulsed illumination source and electronically gated image intensifier. Accurate control of the delay period and efficient detection of the faint fluorescence are critical tasks that have been approached in various ways by different groups [7–10]. Most modern time-resolved fluorescence microscopy (TRFM) designs employ a gated microchannel plate (MCP) image intensifier to meet this requirement since it provides both high optical gain and excellent temporal resolution. The MCP intensifier is a compact array of microscopic photomultiplier channels that can be electrically gated with nanosecond precision. A phosphor target is used to convert the amplified signal into a visible image for collection by a charge-coupled device (CCD) camera.

Long lifetime fluorescent chelates suitable for TRFM are largely based on the trivalent lanthanides, terbium^{3+} and europium^{3+} [11–15].

The intrinsic absorbance of europium and terbium is very low (< 1 M^{-1} cm^{-1}) and this is offset by chelating the ion with a sensitizing ligand to capture and transfer energy [16]. The recent report of a highly fluorescent chelate [17] led us to synthesize a derivative for use in the evaluation of time-resolved techniques on our TRFM.

Methods to produce a pulsed light source include motor-driven chopper wheels, acousto-optical modulators (AOMs), pulsed lasers or flashlamps [7,18–20]. Mechanical choppers that interrupt the excitation beam have been favored for a number of years due to their low cost, free choice of excitation source and high repetition rate. When compared to flashlamps however, their poor beam quality, slow switching rates and mechanical vibration are significant limitations. Specifically, we have found that vibration is problematic with microbial applications, which typically require high magnification. With these considerations in mind, a design based on a fast flashlamp and single stage image intensifier has been employed.

TRFM techniques greatly assist resolution of target cells from background autofluorescence since emissions from autofluorescent life-forms and debris are eliminated from the field of view by virtue of their short fluorescent lifetimes. Thus TRFM has applications where autofluorescence limits the utility of fluorescence-based techniques [3,21–23].

We describe the detection of *Giardia lamblia* cysts in an environmental water sample that contained large amounts of autofluorescent material. The cysts were detected using an immunofluorophore conjugate with a long fluorescent lifetime. This model system was used to examine the efficiency of TRFM to resolve target cells from autofluorescent background. To our knowledge, this is the first report of the use of TRFM in a microbiological application.

2. Materials and methods

2.1. Instrumentation

The configuration of the time-resolved microscope is shown in Fig. 2. Within the Dicam-Pro camera head (PCO Computer Optics, Kelheim, Germany) is an image intensifier coupled to a CCD camera. The image intensifier is a single stage 12-μm MCP array fitted with a gating module to control image acquisition to 5 ns resolution. The cooled monochrome CCD element is a super VGA 1280(H)×1024(V) format that supports 12-bit (4096 gray scales) resolution. An image capture-manipulation software package together with drivers and software for the PCI card were supplied.

2.2. Oriel flashlamp power supply

An Oriel model 68825 power supply was used to control a 6426 guided-arc xenon flashlamp with repetition rates up to 100 Hz. Maximum flash energy was 160 mJ at 60 Hz with discharge duration of 1.6 μs full width half maximum (FWHM). Trigger input is accessible from a rear connector together with a synchronization output for the camera.

2.3. Microscope

A Zeiss Axioplan epifluorescence microscope equipped with a 50-W Hg vapor lamp was retrofitted with a dual illumination port adapter to accommodate the Oriel flashlamp. The illumination source could then conveniently be switched to the flashlamp for time-resolved studies or mercury lamp for conventional epifluorescence microscopy. Zeiss filter set 487909-0000, referred to in the text as filter set 9, is recommended for use with fluorescein (FITC) labels and was used for conventional microscopy. A custom filter set comprised of a BP340/10 excitation filter, FT560 beam splitter and BP575-640 emission filter was used for time-resolved microscopy. Images were captured using a 40× Neophot objective and 10× camera adapter mount to give a final magnification of 400.

2.4. Host PC software

Custom software was written to integrate a camera control library (PCO Computer Optics, Kelheim, Germany) with an image-handling library from Accusoft Corporation (Northborough, MA, USA). The package also supported statistical functions to analyze selected regions of

captured images. Software was added to communicate over the host PC's serial port with an external microcontroller that controlled an on-board solid-state relay for triggering the flashlamp. Flash count and duration between flashes were fully programmable from software dialogs within the application.

2.5. Water sample

G. lamblia cysts (5.7×10^4) were added to 10 μl of water concentrate equivalent to 100 ml of environmentally sourced water [27]. The 10 000:1 concentrate used was rich in autofluorescent algae, diatoms, plant debris and fluorescent minerals.

2.6. Fluorescent substrates

TruCOUNT beads (Becton Dickinson, Sydney, Australia) 6 μm in diameter were suspended in 100 μl of 0.02 M phosphate-buffered saline (PBS) and a 5-μl volume used for slide preparations.

The beads are reported to display a sub-microsecond fluorescence lifetime and are optimally excited by 480 nm light (Davis, K., Becton Dickinson Inc., personal communication). PBS was prepared with a single Aldrich P-4417 tablet in 100 ml de-ionized water, pH set to 6.8 with 1 M HCl. The published method [26] was used as the basis for the synthesis of a fluorescent europium chelate: 4,4′-bis-(1″,1″,1″,2″,2″,2″-pentafluoro-4″,6″-pentandion-6″-yl)-chlorosulfo-*o*-terphenyl (BPPCT).

2.7. Antibody–chelate conjugation

A 100-μl aliquot of *G. lamblia* IgG antibody G203 (Ausflow Pty. Ltd., Sydney, Australia) at 2.2 mg ml^{-1} concentration was desalted, exchanged for 0.1 M bicarbonate buffer at pH 9.25 and concentrated two-fold using Millipore Ultrafree-0.5 50 K centrifugal filters. The concentrated antibody (4.4 mg ml^{-1}) in 50-μl volume was reacted with 10 μl of BPPCT dissolved in DMF at a concentration of 25 mg ml^{-1}. BPPCT was added as two (5 μl) aliquots separated by 1 h for a total reaction time of 2 h at room temperature. Removal of unconjugated material and buffer exchange was achieved by three washes in 50 K centrifugal filters using PBS. Fluorescence to protein ratio (F/P) was determined as 8.5 based on the extinction coefficient (ε_{320}) of BPPCT (3.84×10^4 cm^{-1} M^{-1}). G203 antibody has a negligible absorption at 320 nm so the observed A_{280}/A_{320} ratio of BPPCT (0.65) was used to determine protein concentration.

Protein concentration (mg ml^{-1}) = $(A_{280} - (A_{320} \times (A_{280}/A_{320}))) \times A_{prot320}$, where $A_{prot320}$ is the absorbance at 320 nm for antibody at 1 mg ml^{-1} (a value of 1.34 was used).

The immunofluorophore was stable for 4 weeks, stored at 4°C and was filtered before use with Millipore Ultrafree MC filters 0.22 μm.
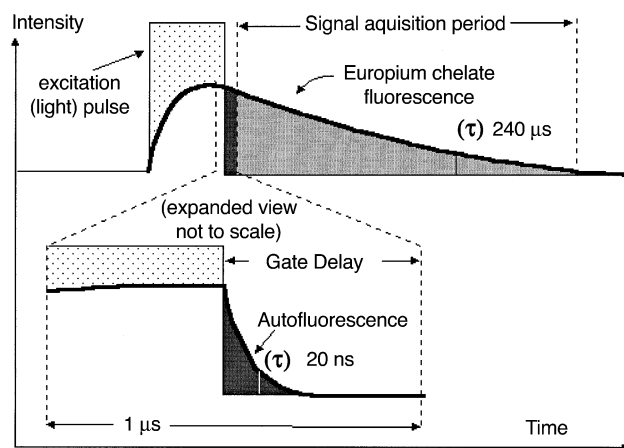

Fig. 1. The light pulse induces fluorescence from autofluorophores and the euoropium chelate alike. Termination of the light pulse is followed by the rapid decay of autofluorescence whereas fluorescent intensity of the chelate decays thousands of times more slowly. Signal acquisition is held off for the gate delay period to permit decay of prompt autofluorescence, light from the luminescing chelate is then gathered minus the background.

G. lamblia cysts were labeled using antibody at concentrations ranging from 28 μg ml^{-1} to 280 μg ml^{-1} and optimal brightness was achieved at 33 μg ml^{-1} (data not shown). The spiked *G. lamblia* water sample of 10 μl was filtered on a Millipore Isopore 0.8-μm membrane filter. Triple washing of the filter with 200 μl of PBS was followed by incubation for 15 min with 100 μl of G203 chelate conjugate antibody at 33 μg ml^{-1} in PBS buffer. Filters were washed several times with 200 μl of PBS before chelate activation using 100 μl of 2 mmol EuCl$_3$ solution for 5 min followed by a further three washes with PBS. Filter concentrates were washed from the membrane using PBS and collected for slide preparation.

2.8. Lifetime determination

The characteristic time that a fluorescent molecule remains in the excited state prior to returning to the ground state is known as the fluorescent lifetime (τ). Assuming single exponential fluorescence decay, the intensity of the fluorescence at time T may be defined using Eq. 1:

$$I_T = I_0 \cdot e^{T/-\tau} \tag{1}$$

where the pre-exponential constant I_0 is the initial intensity immediately after excitation and τ is the fluorescence lifetime. The fluorescence lifetime equates to the time taken for intensity to decay to approximately 37% of the original intensity (e^{-1}). Measurement of this parameter is important to quantitatively determine the effectiveness of the TRFM in reducing the effect of autofluorescence. Lifetime of selected regions in the field of view was determined by logging fluorescence intensity measurements over increasing gate delay periods and fitting to Eq. 1

using Origin 6.0 software (Microcal Software Inc., Northampton, MA, USA).

2.9. Image processing

An average intensity value for regions of interest within the captured image was determined by sampling a rectangular region containing 600–1000 pixels. The running average of four such samples was the value logged. Software written for the TRFM included a line histogram tool that captured position and intensity values for all pixels between any two points selected by the operator (see Fig. 3 for example). This tool was used to capture data sequences for processing by Origin 6.0 to generate the three-dimensional (3D) graph shown in Fig. 4. The contrast improvement achieved using time-resolved techniques was calculated using the ratio (Eq. 2) of the fluorescence intensity for labeled cysts (I_C) and background (I_B) without time resolution (I_{C0}/I_{B0}) and after 60 μs (I_{C60}/I_{B60}):

$$\Delta \text{Contrast} = (I_{C60}/I_{B60})/(I_{C0}/I_{B0}) \qquad (2)$$

Images were processed to improve printing clarity by a brightness-boosting algorithm (Accusoft library) after determination of the change in contrast (ΔContrast).

3. Results

3.1. Time-resolved image capture

The monochrome sequence shown in Fig. 3 illustrates qualitatively the effectiveness of time-resolved techniques using a delay duration of 10 μs and 60 μs. The two *Giardia* cysts (labeled A and B) in the field of view could be resolved with increased contrast from background using a 10-μs delay. The initial intensity of some autofluorescing debris exceeded the brightness range employed for the capture. However after 10 μs, the labeled cysts were the brightest objects in the field of view. Increasing the gate delay to 60 μs resulted in a small loss in the visible intensity of the cysts yet this was greatly offset by a large
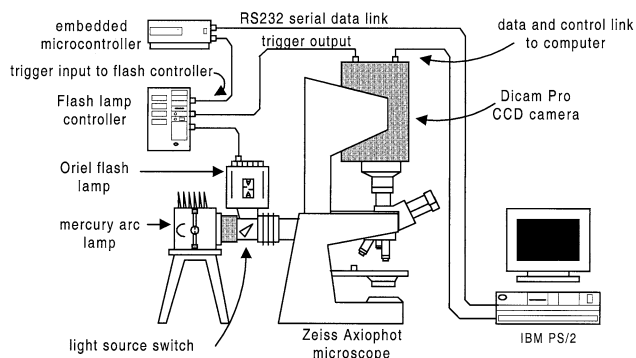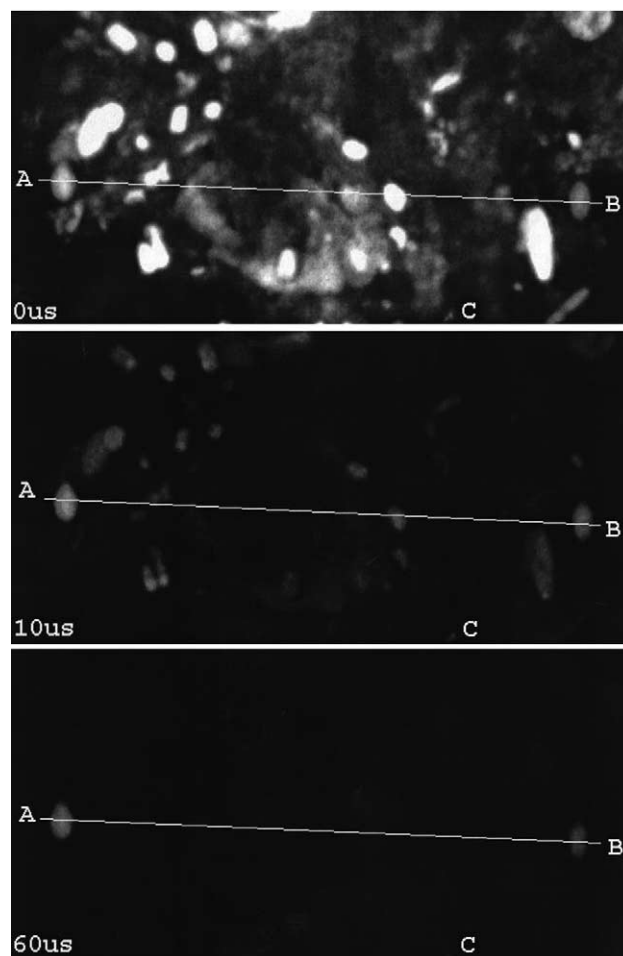

Fig. 3. Two *Giardia* cysts labeled A and B embedded in a highly autofluorescent background. Top image captured using Zeiss filter set 09, 40× objective, 10× eyepiece and no time delay. Middle and lower images captured in time-resolved mode (using the TR filter set) at 10 μs and 60 μs respectively by integrating 250 capture loops. The particle labeled C was determined to be a fragment of precipitated immunofluorophore conjugate.

reduction in background and could be compensated for by increasing photomultiplier gain.

Quantitative analysis of cyst 'A' contrast using the line histogram software indicated a 30-fold enhancement achieved with a gate delay of 60 μs relative to no delay (0 μs). Fig. 4 serves to highlight the large difference in observed fluorescent lifetimes for autofluorescent and chelate labeled species. Autofluorescence is reduced to the level of instrument background noise from 60 μs onwards and implies a potential limit in contrast ratios to approximately 50-fold based on the 2% noise figure measured. Optimal S/N performance was achieved by extending the time delay until background reached this noise floor. Further extension served only to decrease chelate emission without a corresponding gain in contrast. Coordinates 50 and 300 on the *X*-axis in Fig. 4 specify the points used to determine lifetime coefficients for background and label respectively. These points correspond to the center of the

Fig. 2. Layout of the instrumentation used in the time-resolved fluorescence microscope.
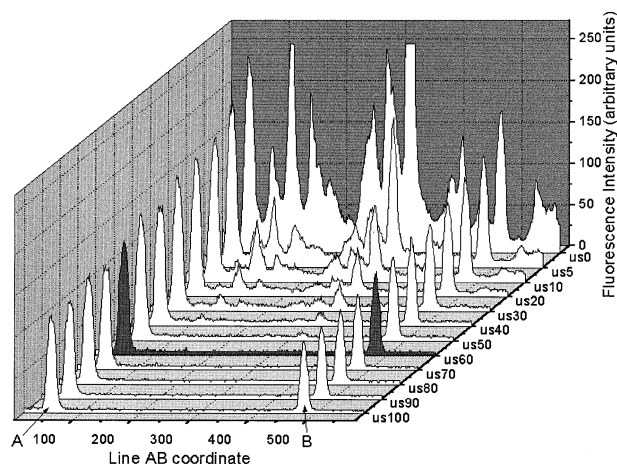
Fig. 4. 3D cascade plot illustrating decay of fluorescence intensity over time for immunoconjugate and autofluorophores in Fig. 3. The X-axis corresponds to the line A–B separating two labeled cysts in Fig. 3. Time and fluorescence intensity correspond to the Z- and Y-axes respectively.

cyst labeled A and a bright autofluorescing component visible just past half way on the line A–B in Fig. 3 (0 μs).

Chelate labeled cysts in 0.02 M PBS (pH 6.8) displayed a fluorescence lifetime (τ) of 242 ± 38 μs with a correlation coefficient of 0.87 between experimental data and predicted single exponential decay estimates (Oriel 6.0 software). Experimentally determined lifetime for background autofluorescence excited by 350 nm wavelengths (X-coordinate 300 in Fig. 4) was 19 ± 0.7 μs. The correlation coefficient relating predicted and experimentally determined autofluorescence lifetime was 0.98. Measurements in time-resolved mode using Zeiss filter set 09 to excite emission from 6-μm TruCOUNT beads (data not shown) gave an estimated lifetime of 19 ± 1 μs with a correlation coefficient of 0.99.

4. Discussion

Fluorescence microscope techniques are extensively used in microbial ecology, as they are amongst the most useful methods for the study of individual microorganisms in environmental samples [1,3,24]. Fluorescence signal strength against an autofluorescent background is a critical factor in determining the utility of such methods and many environmental samples contain sufficient autofluorescing material to limit the use of fluorescent-based techniques. With the TRFM, a progressive reduction in autofluorescence was achieved as the delay between the excitation flash and image acquisition was increased. Fluorescence intensity of labeled cysts decreased only minimally in the same time frame and image contrast was consequently greatly enhanced. Overall, reduction of autofluorescence resulted in a 30-fold increase in S/N ratio for labeled cysts against background.

The TRFM has been shown to greatly aid the detection

of a specific microorganism in an environmental sample using immunofluorescent techniques. The technique has many potential applications in microbial ecology where the fluorescence signal strength relative to background autofluorescence limits the utility of conventional fluorescence microscopy. For example, it is possible to link long-lived fluorophores to oligo-nucleotide probes and perform time-resolved FISH [12,25–28]. This would facilitate the direct detection of microorganisms using FISH techniques where currently signal strengths relative to autofluorescent background limit the application [4,5,29,30].

TRFM results in images with vastly decreased complexity and this facilitates the use of automated computer recognition systems that can process images at high speed. Repetitive and tedious analyses can be allocated to an automated system that requires minimal operator intervention.

Two essential components of the TRFM are the image capture system and pulsed light excitation source. The optimal excitation pulse/acquisition cycle is illustrated in Fig. 1 and the acquisition timing of the TRFM is close to ideal. The Dicam-Pro CCD camera can be gated with nanosecond accuracy and the integrated image intensifier provides sufficient gain (10 000-fold) to capture weak fluorescence. Alternatives to an electronically gated image intensifier require some method of optically blocking the excitation beam, and motor-driven chopper wheels or ferro-electric liquid crystal display (LCD) shutters have been used. Mechanical choppers are slow, vibration prone and degrade acquisition efficiency whilst LCD shutters have poor optical transparency [12,18–20]. Most modern TRFM designs opt for the superior performance offered by image-intensified gated CCDs.

Arc-lamps are the brightest continuous radiation sources available excluding lasers, however they require some means of interrupting the beam to produce a pulsed excitation source. AOMs or chopper wheels have been used for this purpose although this adds significantly to the cost and complexity of the final instrument [7,12,18,19]. Furthermore, the synchronization issues and vibration problems associated with motor-driven choppers can be difficult to overcome. Lasers have been employed in some advanced TRFM designs and the excitation pulse is often generated by a tunable dye-laser pumped by a larger laser [7,8,32]. Such systems deliver high-energy pulses with near ideal excitation characteristics but cost is high and usually only justified for specialized applications.

Flashlamps have higher peak irradiance and relatively more energy available in the ultra-violet (UV) portion of the spectrum than arc-lamps [31]. This is important since europium and terbium chelates both require excitation in the mid-UV (320–350 nm). Pulse width of the flash measured at FWHM can be less than 1 μs for selected commercial flashlamps, although the trailing edge at lower intensities extends for a much longer period. The apparent persistence of autofluorescence for up to tens of micro-

seconds is an artifact induced by the slow decay of flash-lamp plasma. Different spectral components in the plasma decay at different rates with short wavelengths reported to decay most rapidly [31]. Fluorescent TruCOUNT beads were used to determine plasma lifetime since they are known to have a sub-microsecond fluorescence lifetime.

Flashlamp energy was determined to decay at an approximately single exponential rate with a lifetime of 19 μs. This equates to a residual flash intensity after 60 μs of 4% of initial intensity whereas the chelate (lifetime of 242 ± 38 μs) retained 88% of its original intensity.

Whilst the flashlamp is not perfect due to relatively slow decay of the excitation pulse, this is not a significant problem when used in conjunction with a fluorophore having a fluorescence lifetime at least 10-fold greater than total flash lifetime.

The flashlamp-based TRFM described here is devoid of the vibration often associated with conventional mechanical TRFMs [33] and is significantly faster and less costly than arc-lamps/chopper configurations. Moreover, flashlamp life is reported to exceed 10^8 flashes.

The availability of suitable fluorescent chelates has been a significant factor in limiting the application of TRFM. Early attempts to prepare immunoconjugates using commercial fluorophores such as Quantum Dye (Research Organics Inc., Cleveland, OH, USA) met with no success and prompted the synthesis of a number of chelates reported in the literature. In our experience, the BPPCT fluorophore has superior fluorescence intensity over quinolinone- [15] and phenanthroline- [34] based chelates prepared, and conjugation to antibodies presented few difficulties. Perkin Elmer (Wellesley, MA, USA) supplies long-lived fluorescent labels (LANCE reagents) that are marketed for time-resolved work. Carbostyril 124 is available commercially from Aldrich and when modified with a chelating side-arm has been reported to be a suitable fluorophore for TRFM [15,16,19,35]. Fragments of precipitated immunoconjugate, as typified by the particle labeled C in Fig. 3, were observed in some fields of view. Filtration of the immunoconjugate is necessary to remove these fragments since they constitute non-specific background, however precipitation can occur during the incubation of immunoconjugate with sample. We have found that stability of the antibody (and resistance to precipitation) is inversely related to the level of bound fluorophore (data not shown). Precipitation can be minimized through use of fresh preparations of the immunoconjugate and avoiding heavy labeling (F/P ratio > 8). The hydrophobic nature of BPPCT increases the tendency of the antibody to precipitate so that optimization of the conjugation protocol (by varying BPPCT concentration) is necessary for best results.

The TRFM as configured can deliver a 30-fold contrast enhancement of labeled target against background. Other systems have been reported to deliver higher S/N ratios, however this was achieved at the expense of an AOM equipped laser light source [7]. Decreasing the flash life-time or increasing label quantum yield both improve the S/N ratio and we are currently investigating the latter approach. Enzyme-linked amplification strategies have been used with great success to increase the amount of bound time-resolvable fluorophore and significantly boost detection thresholds [26]. These methods rely on the deposition of biotin at the target site that is then subsequently bound to streptavidin conjugated with time-resolvable fluorophore.

We have shown that a relatively simple design for a lab-built TRFM based on a fast flashlamp and image-intensified camera can greatly reduce autofluorescence when used with an appropriate fluorophore. The reduction in autofluorescence is achieved with a concomitant 30-fold increase in contrast that can easily be improved by enhancements to the fluorophore or excitation source.

References

[1] Nath, J. and Johnson, K.L. (2000) A review of fluorescence *in-situ* hybridization (FISH): Current status and future prospects. Biotech. Histochem. 75, 54–78.

[2] Rodgers, M.R., Flanigan, D.J. and Jakubowski, W. (1995) Identification of algae which interfere with the detection of *Giardia* cysts and *Cryptosporidium* oocysts and a method for alleviating the interference. Appl. Environ. Microbiol. 61, 3759–3763.

[3] Veal, D., Deere, D., Ferrari, B., Piper, J. and Atfield, P. (2000) Fluorescence staining and flow cytometry for monitoring microbial cells. J. Immunol. Methods 243, 191–210.

[4] Mounteer, A.H., Passos, F.M.L., Borges, A.C. and Silva, D.O. (2002) Detecting structural and functional differences in activated sludge bacterial communities originating from laboratory treatment of elementally and totally chlorine-free bleaching effluents. Can. J. Microbiol. 48, 245–255.

[5] Nishiyama, M., Shiomi, Y. and Marumoto, T. (1997) Application of rRNA-based probe for detection of a bacterium in rhizoplane. Soil Sci. Plant Nutr. (Tokyo) 43, 749–755.

[6] Condrau, M.A., Schwendener, R.A., Niederer, P., Anliker, M., Zimmermann, M., Muser, M.H. and Graf, U. (1994) Time-resolved flow cytometry for the measurement of lanthanide chelate fluorescence: Ii. Instrument design and experimental results. Cytometry 16, 195–205.

[7] Hennink, R.J., de Haas, R., Verwoerd, N.P. and Tanke, H.J. (1996) Evaluation of a time-resolved fluorescence microscope using a phosphorescent Pt-porphine model system. Cytometry 24, 312–320.

[8] Periasamy, A., Wodnicki, P., Wang, X.F., Kwon, S., Gordon, G.W. and Herman, B. (1996) Time-resolved fluorescence lifetime imaging microscopy using a picosecond pulsed tunable dye laser system. Rev. Sci. Instrum. 67, 3722–3731.

[9] Rulli, M., Kuusisto, A., Salo, J., Kojola, H. and Simell, O. (1997) Time-resolved fluorescence imaging in islet cell autoantibody quantitation. J. Immunol. Methods 208, 169–179.

[10] de Haas, R., van Gijlswijk, R.P.M., van der Tol, E.B., Zijlmans, H.J.M.A.A., Bakker-Schut, T., Bonnet, J., Verwoerd, N.P. and Tanke, H.J. (1997) Platinum porphyrins as phosphorescent label for time-resolved microscopy. J. Histochem. Cytochem. 45, 1279–1292.

[11] Yuan, J., Wang, G., Kimura, H. and Matsumoto, K. (1997) Highly sensitive time-resolved fluoroimmunoassay of human immunoglobulin E by using a new europium fluorescent chelate as a label. Anal. Biochem. 254, 283–287.

[12] Seveus, L., Vaisala, M., Syrjanen, S., Sandberg, M., Kuusisto, A., Harju, R., Salo, J., Hemmila, I., Kojola, H. and Soini, E. (1992) Time-resolved fluorescence imaging of europium chelate label in immunohistochemistry and *in-situ* hybridization. Cytometry 13, 329–338.

[13] Selvin, P.R. and Hearst, J.E. (1994) Luminescence energy transfer using a terbium chelate: Improvements on fluorescence energy transfer. Proc. Natl. Acad. Sci. USA 91, 10024–10028.

[14] Diamandis, E.P., Morton, R.C., Reichstein, E. and Khosravi, M.J. (1989) Multiple fluorescence labeling with europium chelators. Application to time-resolved fluoroimmunoassays. Anal. Chem. 61, 48–53.

[15] Chen, J. and Selvin, P.R. (2000) Synthesis of 7-amino-4-trifluoromethyl-2-(1H)-quinolinone and its use as an antenna molecule for luminescent europium polyaminocarboxylates chelates. J. Photochem. Photobiol. 135, 27–32.

[16] Selvin, P.R., Jancarik, J., Li, M. and Hung, L. (1996) Crystal structure and spectroscopic characterization of luminescent europium chelate. Inorg. Chem. 35, 700–705.

[17] Yuan, J. and Matsumoto, K. (1998) A new tetradentate β-diketonate-europium chelate that can be covalently bound to proteins for time-resolved fluoroimmunoassay. Anal. Chem. 70, 596–601.

[18] Verwoerd, N.P., Hennink, E.J., Bonnet, J., Van der Geest, C.R.G. and Tanke, H.J. (1994) Use of ferro-electric liquid crystal shutters for time-resolved fluorescence microscopy. Cytometry 16, 113–117.

[19] Vereb, G., Jares-Erijman, E., Selvin, P.R. and Jovin, M.T. (1998) Temporally and spectrally resolved imaging microscopy of lanthanide chelates. Biophys. J. 74, 2210–2222.

[20] Phimphivong, S. and Saavedra, S.S. (1998) Terbium chelate membrane label for time-resolved, total internal reflection fluorescence microscopy of substrate adherent cells. Bioconjug. Chem. 9, 350–357.

[21] Ferrari, B.C., Vesey, G., Davis, K.A., Gauci, M. and Veal, D. (2000) A novel two-colour flow cytometric assay for the detection of *Cryptosporidium* in environmental water samples. Cytometry 41, 216–222.

[22] McKay, J.A., Murray, G.I., Keith, W.N. and McLeod, H.L. (1997) Amplification of fluorescent *in-situ* hybridization signals in formalin fixed paraffin wax embedded sections of colon tumor using biotinylated tyramide. Mol. Pathol. 50, 322–325.

[23] Vesey, G., Deere, D., Gauci, M., Griffiths, K.R., Williams, K. and Veal, D. (1997) Evaluation of fluorochromes and excitation sources for immunofluorescence in water samples. Cytometry 29, 147–154.

[24] Mullins, J.M. (1999) Overview of fluorochromes. Methods Mol. Biol. 115, 97–105.

[25] Sueda, S., Yuan, J. and Matsumoto, K. (2000) Homogeneous DNA hybridization assay by using europium luminescence energy transfer. Bioconjug. Chem. 11, 827–831.

[26] de Haas, R.R., Verwoerd, N.P., Van Der Corput, M.P., Van Gijlswijk, R.P., Siitari, H. and Tanke, H.J. (1996) The use of peroxidase-mediated deposition of biotin-tyramide in combination with time-resolved fluorescence imaging of europium chelate label in immunohistochemistry and *in-situ* hybridization. J. Histochem. Cytochem. 44, 1091–1099.

[27] Hakala, H. and Lonnberg, H. (1997) Time-resolved fluorescence detection of oligonucleotide hybridization on a single microparticle: Covalent immobilization of oligonucleotides and quantitation of a model system. Bioconjug. Chem. 8, 232–237.

[28] Li, M. and Selvin, P.R. (1997) Amine-reactive forms of a luminescent diethylentriamepentaacetic acid chelate of terbium and europium: Attachment to DNA and energy transfer measurements. Bioconjug. Chem. 8, 127–132.

[29] Macdonald, R. and Brozel, V.S. (2000) Community analysis of bacterial biofilms in a simulated recirculating cooling-water system by fluorescent *in-situ* hybridization with rRNA-targeted oligonucleotide probes. Water Res. 34, 2439–2446.

[30] Schonhuber, W., Zarda, B., Eix, S., Rippka, R., Herdman, M., Ludwig, W. and Amann, R. (1999) *In-situ* identification of cyanobacteria with horseradish peroxidase-labeled, rRNA-targeted oligonucleotide probes. Appl. Environ. Microbiol. 65, 1259–1267.

[31] Esposito, E., Fernandes, N., FitzSimons, C. and Marino, E.I. (1994) Light sources, monochromators and spectrographs, detectors and detection systems and fiber optics. Oriel Corporation. Vol. 2, pp. 1–148.

[32] Konig, K., So, P.T.C., Mantulin, W.W., Tromberg, B.J. and Gratton, E. (1996) Two-photon excited lifetime imaging of autofluorescence in cells during UVA and NIR photostress. J. Microsc. 183, 197–204.

[33] Lovgren, T., Heinonen, P., Lehtinen, P., Hakala, H., Heinola, J., Harju, R., Takalo, H., Mukkala, V.-M., Schmid, R., Lonnberg, H., Pettersson, K. and Iitia, A. (1997) Sensitive bioaffinity assays with individual microparticles and time-resolved fluorometry. Clin. Chem. 43, 1937–1943.

[34] Evangelista, R.A., Pollak, A., Allore, B., Templeton, E.F., Morton, R.C. and Diamandis, E.P. (1988) A new europium chelate for protein labelling and time-resolved fluorometric applications. Clin. Biochem. 21, 173–178.

[35] Chen, J. and Selvin, P.R. (2000) Lifetime-and color-tailored fluorophores in the micro- to millisecond time regime. J. Am. Chem. Soc. 122, 657–660.